Mechanics & Industry **21**, 503 (2020)
© AFM, EDP Sciences 2020
https://doi.org/10.1051/meca/2020059

Mechanics & Industry

Available online at:
www.mechanics-industry.org

Regular Article

Effects of process parameters on tensile strength of friction stir welded Al-Cu double-layer sheets

Mohammad Taghizadeh Tabrizi, Amirhossein Jabbari Mostahsan, and Mohammad Sedighi*

School of Mechanical Engineering, Iran University of Science and Technology, Tehran, Iran

Received: 21 September 2019 / Accepted: 19 June 2020

Abstract. In this paper, friction stir welding (FSW) process was used to join double-layer sheets of pure copper and 1050 aluminum alloy produced by explosive welding (EXW). The double-layer sheets were arranged side by side to perform friction stir butt-welding. In this regard, rotary FSW tools with different geometries were used at rotational speeds of 800 and 1250 rpm and linear speeds of 8, 12, and 20 mm min^{-1}, in one and two number of passes. According to the results, the sample welded by a conical tool with a rotational speed of 800 rpm and a linear speed of 12 mm min^{-1} in one pass offered the highest tensile strength, which was approximately equivalent to the 84% of the strength of the raw double-layer sheet. In addition, applying the second FSW pass and using a threaded tool from the aluminum side had negative effects on the tensile strength. The microstructural evaluation showed the presence of more intermetallic phases including Al_4Cu_9, AlCu, and Al_2Cu in the sample welded by the threaded tool from the aluminum side in two number of passes, which was the responsible of the lower tensile strength and the higher microhardness.

Keywords: friction stir welding / double-layer sheet / aluminum-copper / explosive welding / tensile strength

1 Introduction

Friction stir welding (FSW) is one of the solid state welding methods that was introduced in 1991. Nowadays, it is widely used to connect a variety of materials, especially dissimilar metals. This technique not only does not have the limitations of fusion welding methods, but also has many advantages, including the possibility of binding metals with different melting points [1,2]. In this process, a rotational non-consumable tool penetrates into the welding line. Then, materials around the tool converted to semi-solid form due to the heat generated by friction. Next, the welding tool starts to move forward and, in this situation, it mixes and forges both semi-solid materials around itself.

In FSW, the presence of turbulence in the semi-solid metals and heat generated in the weld nugget causes changes in the microstructure of the materials in the areas around and in the center of the welding line, including grain refinement and formation of precipitations [3–5]. Also, a similar process can be used in order to refine the microstructure or distribute reinforcing particles in a base metal [6,7]. According to the definition of the process, the weld zone is divided to four distinct areas after welding. The mentioned areas are defined based on the applied temperature or mechanical work on those areas [8]. The structure of base metal zone (BZ), which is slightly far from the welding site, remains unchanged since it is not affected by any mechanical or thermal factors. The next region is the heat affected zone (HAZ). This region is the first changed zone after BZ, which is only affected by the thermal cycles. The thermo-mechanically affected zone (TMAZ) is located between the weld nugget and the HAZ. This zone is affected by plastic deformation induced by the tools and also tolerates the thermal cycles. The stir zone (SZ) is a region, which is changed mechanically and thermally by the tool used in the process. In this region, the grains and microstructure of the base metals are completely affected by the welding process.

A serious problem in fusion welding of Cu and Al alloys, even when a well joint is obtained, is the undesirable change of the microstructure, leading to a sharp drop in the tensile strength and ductility. However, there is an ability to prevent significant changes in the microstructure and the mentioned mechanical properties by performing FSW in the solid state condition [9]. Farahati et al. [10] studied the effect of various rotational speeds on butt joint FSW of dissimilar aluminum 1050 and commercial copper sheets. The results showed that welding at a rotational speed of 1250 rpm results in the best mechanical properties, while increase of this speed would decrease the mechanical properties. Xue et al. [11] investigated the effect of sheets

* e-mail: sedighi@iust.ac.ir

Table 1. The chemical composition of base metals (weight percentage).

AA 1050	**Al**	**Si**	**Fe**	**Cu**	**Mn**	**Mg**	**Zn**	**Ti**	**V**	**Others**
	Base > 99.5	< 0.25	< 0.40	< 0.05	< 0.05	< 0.05	< 0.05	< 0.03	< 0.05	< 0.03
Copper	**Cu**	**Zn**	**Pb**	**Sn**	**P**	**Ni**	**Co**	**Ag**	**Fe**	**Others**
	Base > 99.9	< 0.01	< 0.01	< 0.01	0.01	0.01	0.02	0.005	< 0.005	< 0.01

position and tool rotation direction in the lap joint FSW of aluminum 1060 and copper sheets. According to their results, placing the aluminum sheet on the copper and implementing the welding on the aluminum side will improve the mechanical properties of the joint. Li et al. [12] studied the microstructure and mechanical properties of the butt joint FSW of aluminum 1350 and copper with the deviation of the welding tool toward the aluminum side. The obtained results exhibited the lack of intermetallic compounds and an increase in the relative hardness in the lower parts of the joint. Bisadi et al. [13] investigated the effect of tool speeds on the microstructure and mechanical properties of aluminum 5083 and copper lap joint FSW. According to the results, heat generated in the weld nugget significantly influences on the apparent qualities and visible defects. Moreover, the ultimate tensile strength (UTS) is reduced by increasing the inlet generated heat. Galvao et al. [14] studied the effect of the aluminum alloy types (5083 and 6082) on the lap joint of Al-Cu using FSW. The results exhibited that there were many defects in the weld of aluminum 5083 and copper, while two metals was uniformly mixed in the weld of aluminum 6082 and copper. Barekatain et al. [15] investigated the mechanical properties and the microstructure of butt joint FSW of aluminum 1050 and copper sheets using annealing process and constrained groove pressing (CGP) method. A relative decrease in the hardness of CGP welded sheets was observed compared to those welded by the annealing process. Akinlabi et al. [16] studied the effects of FSW parameters on the corrosion properties of aluminum 5754 and copper butt welding. According to the results, corrosion resistance was improved by increasing the rotational speed. Sadeghi et al. [17] investigated the mechanical properties of the aluminum 1050-copper joint, using FSW method. The results indicated the effect of higher rotational speeds on the creation of a wider mixing zone. Moreover, increasing the welding time enhanced the diffusion of the atoms into the mixing zone and consequently increased the formation of intermetallic compounds. Anbukkarasi et al. [18] improved the strength and the ductility of AA2024-Cu FSW joints using zinc strips as an interlayer material.

Double-layer sheets have many applications in automotive, aviation and chemical industries. In fact, they can benefit from various and complementary properties of both sheets such as low density, high strength and ductility, improved corrosion resistance, and desirable thermal and electrical properties [19]. Furthermore, they can use the existing thermal expansion coefficients difference in order to create targeted mechanical movement. However, to expand the scope of their applications, welding of double-layer sheets is an essential field to study. Although there are many researches about different types of FSW between aluminum and copper sheets, to the best of the authors' knowledge, no study has been done on the friction stir welding of double-layer sheets. The purpose of this paper is to investigate the FSW of aluminum-copper double-layer sheets fabricated by explosive welding. In this regard, the butt welding of the mentioned double-layer sheets has been studied using various parameters including the direction of the tool entrance (from copper or aluminum side), different rotational and traversing speeds of the tool, various tool geometric shapes, and the number of welding passes. For this purpose, tensile strength, hardness, and the microstructure of the different samples have been examined.

2 Materials and experimental method

FSW was performed on the double-layer sheets of 1050 aluminum alloy and 99.9% pure copper. Table 1 shows the chemical composition of these materials.

First, the Al-Cu double-layer sheets were prepared by EXW method using copper and aluminum sheets with a thickness of 2 mm. Then, the sheets were cut to pieces with dimensions of 200 mm × 25 mm. Afterwards, the double-layer sheets were initially cold-rolled without any thickness reduction in order to remove the distortions resulted by EXW. Next, the specimens were subjected to annealing heat treatment at 300 °C for 30 min. The FSW tools were made of hot-work steel alloy AISI-H13 and was hardened up to 48 HRC by an appropriate heat treatment. The tools were made with three geometric shapes of cylindrical, conical, and threaded. Figure 1 shows the geometry of the tools used in this study. The height of the pins and the diameter of the shoulders were considered to be the same for all the tools. The rotational speeds used for the tools were 800 and 1250 rpm with traversing speeds of 6, 12 and 20 mm min^{-1}. Moreover, the tilt angle of the tools was set to 3° from the vertical direction for all the welds. In order to perform the FSW, a milling machine (model FP4MK-4) was employed. It should be noted that regarding the available speeds of the milling machine, the combination of less rotational and higher traversing speeds led to input insufficient generated heat into the welding region. On the other hand, the combination of higher rotational and less traversing speeds increased the temperature significantly, resulting in local melting of the material. Both conditions created some visible defects in the joint.

To investigate the effect of welding parameters, different samples were welded with various conditions. Table 2 shows the different welding parameters applied for the samples. In this regard, six samples were firstly welded with a rotational speed of 800 rpm, a traversing speed of

12 mm min^{-1}, and a tool entrance side from the aluminum layer. Similar conditions were selected by Bisadi et al. [13]. Samples were welded by different tools in one and two passes. For the two-pass welding, since different mechanical properties could be achieved regarding the rotational direction of the tools [20], rotational direction was inversed in the second pass. Based on the results obtained from the tensile tests, the most suitable tool and the number of passes (to achieve the maximum ultimate tensile strength) was used in the next welds. Then, the effect of tool entrance direction (which is aluminum side or copper side) was studied by welding the double-layer sheets with the constant welding parameters and different entrance directions. Finally, various rotational and traversing speeds were applied to weld the samples. It is worth noting to mention that during the FSW of the double-layer sheets with a rotational speed of 800 rpm and a traversing speed of 20 mm min^{-1}, numerous apparent defects were created due to the low generated heat and consequently lack of the necessary materials flow and proper mixing. So, this combination of these speeds was excluded from the experiments.

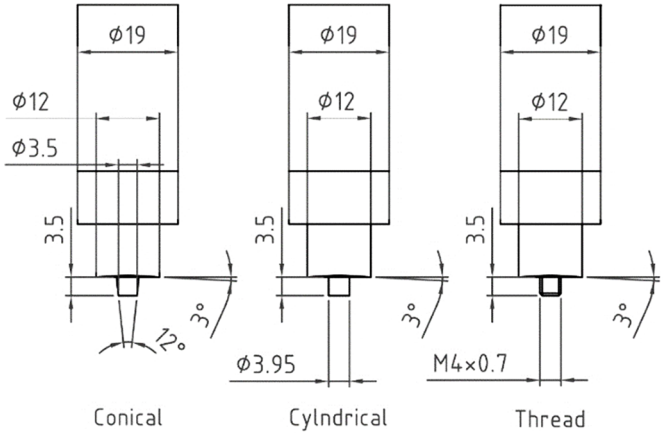

Fig. 1. The geometry of the employed tools.

To evaluate the microstructure and measure the hardness, the welded samples were cut perpendicular to the welding direction. Then, the pieces were mounted and ground by sandpapers with different mesh numbers up to 2500. Finally, they were mechanically polished by alumina powder. The microstructures of the weld nuggets were studied using a scanning electron microscope (SEM) along with energy-dispersive X-ray spectroscopy (EDS). In Vickers microhardness test, the applied force was 200 g for a duration of 10 seconds. To carry out the tensile test, the required specimens were extracted from the welded samples using wire electrical discharge machining. Figure 2 shows the schematic of the FSW process on the

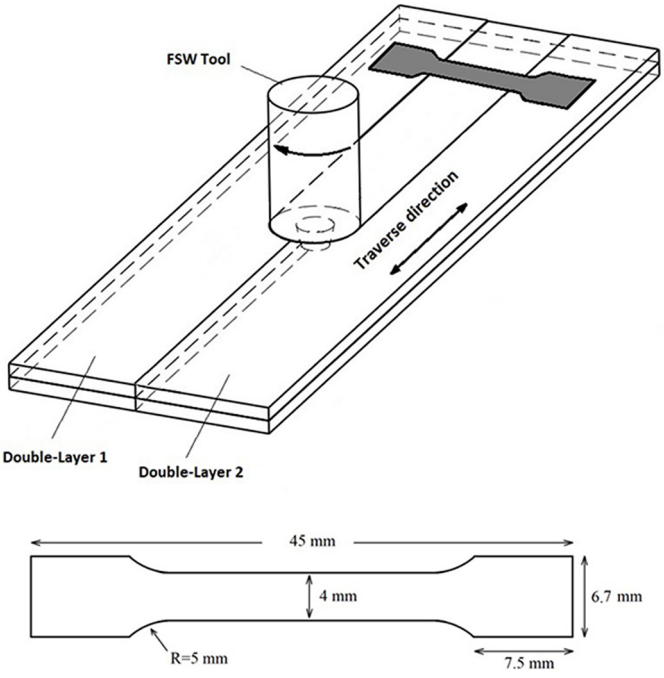

Fig. 2. The schematic of the FSW process and the position and geometry of the tensile test specimens in the welded samples.

Table 2. Different welding parameters applied on the samples.

Sample number	Tool entering side	Tool geometry	Traversing speed (ν)	Rotational speed (ω)	Number of passes (N)
1	Aluminum	Cylindrical	12 mm.min^{-1}	800 rpm	1
2	Aluminum	Threaded	12 mm.min^{-1}	800 rpm	1
3	Aluminum	Conical	12 mm.min^{-1}	800 rpm	1
4	Aluminum	Cylindrical	12 mm.min^{-1}	800 rpm	2
5	Aluminum	Threaded	12 mm.min^{-1}	800 rpm	2
6	Aluminum	Conical	12 mm.min^{-1}	800 rpm	2
7	Copper	Conical	12 mm.min^{-1}	800 rpm	1
8	Copper	Conical	6 mm.min^{-1}	800 rpm	1
9	Copper	Conical	20 mm.min^{-1}	1250 rpm	1
10	Copper	Conical	12 mm.min^{-1}	1250 rpm	1
11	Copper	Conical	6 mm.min^{-1}	1250 rpm	1

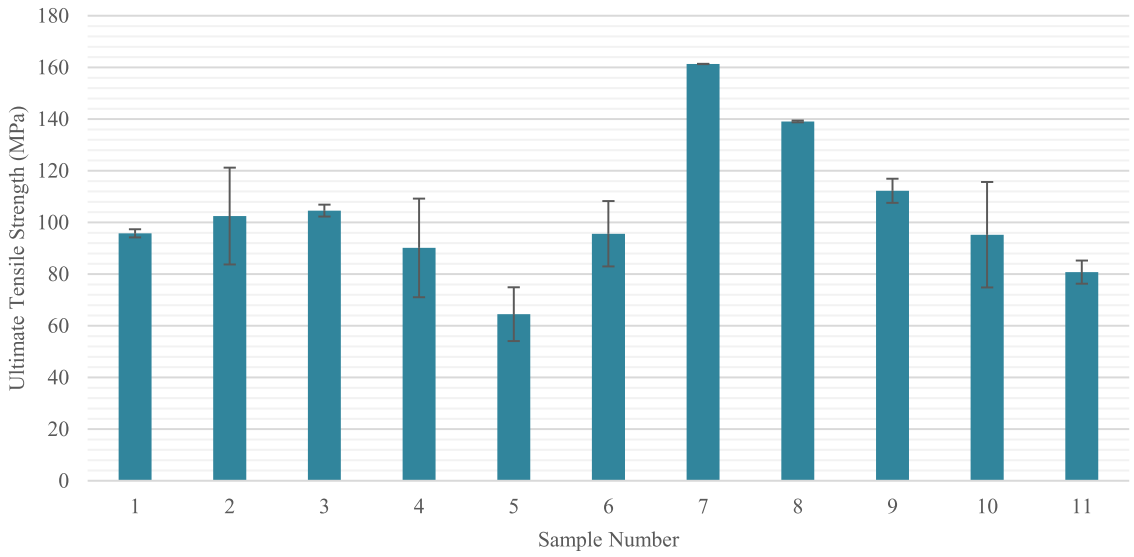

Fig. 3. Ultimate tensile strength of the different samples (the samples numbers are defined in Tab. 2).

double-layer sheets and the position and geometry of the tensile test specimens in the welded samples. The geometry of the specimens was selected according to the ASTM-E8 standard. The speed of the tensile jaws was considered to achieve a strain rate of 0.001 s^{-1}. For each sample, the tensile test was carried out at least two times and the averaged value was reported.

3 Results and discussion

3.1 Tensile test

Ultimate tensile strength is one of the most important parameters to evaluate the quality of a weld joint. The UTS of the different welded samples are illustrated in Figure 3.

In general, samples that were welded by the conical tool offer a higher UTS. In comparison to cylindrical tools, conical tools have the advantage of exerting a downward compressive force that compresses the materials and reduces structural defects. Although the threaded tool can mix two metals more appropriately, it could result in the formation of more brittle intermetallic phases and defects in the Al-Cu joint, degrading the tensile behavior.

Applying the more number of welding passes had a negative effect on the target property. In the other studies, it was observed that increasing the number of passes could decrease the mechanical properties even in a monolithic metal [21]. Since the contact of aluminum and copper at a high temperature for long durations can enhance the possibility of the intermetallic phases formation, more brittle phases would be observed in the samples welded by more number of passes.

In addition to the geometry of the tool and the number of the welding passes, the other important parameter is the entrance side of the tools into the double-layer sheet. Since Al and Cu possess different melting temperatures and also the welding temperature is not constant in the cross section of the sample (area near the shoulder of the tool have a higher temperature), the entrance side can affect the mechanical and microstructural properties of the welded samples. The results indicate the superiority of the sample with the copper entrance side (sample number 7) compared to the sample with aluminum entrance side (sample number 3).

In the next step, the samples were welded with different rotational (6, 12, and 20 mm min^{-1}) and traversing (800 and 1250 rpm) speeds. The results showed that the lower rotational and the higher traversing speeds resulted in a higher ultimate tensile strength. In this regard, the sample number 7 exhibited the highest ultimate tensile strength (161.35 MPa) with a traversing speed of 12 mm min^{-1} and a rotational speed of 800 rpm.

In fact, more rotational and less traversing speeds enhances the generated heat in the welding zone and consequently increases the formation of the brittle intermetallic phases. The presence of these brittle phases increases the microhardness and decreases the maximum strain (which could also affect the ultimate tensile strength). Moreover, inhomogeneity in the weld zone increases the possibility of the micro-crack initiation during the tensile test and as a result, reduces the ductility of the samples. So, the fracture can be happened at the lower stresses, reducing the ultimate tensile strength. In addition, increasing the ratio of the rotational to traversing speeds (ω/v) could cause extra material flashing.

It is also worth noting that the ultimate tensile strength of the annealed raw double-layer sheet before the FSW process was 192.8 MPa. Thus, the maximum UTS of the different welds (UTS of the sample number 7) was achieved approximately 84% of the ultimate strength of the raw double-layer sheet.

By increasing the traversing speed, there is a possibility of generating insufficient heat (low temperature of the process) and inadequate mixing of the materials in the welding region [22]. On the other hand, too much decrease in the traversing speed increases the input heat in the welding point, affecting the amount of intermetallic compounds and welding defects [22]. Likewise, with

increasing the rotational speed, the amount of the input heat is enhanced, which increases the amount of intermetallic compounds and plastic deformation [10,13,17].

In this research, the best and the worst welding conditions were selected by considering the tensile test results. According to Figure 3, the samples number 5 and 7 had the lowest and the highest UTS, respectively. To understand the effects of the welding parameters on the mechanical properties and microstructure of the samples, these two samples were investigated more deeply. Figure 4 illustrates the tensile stress–strain curves of the raw double-layer specimen, sample number 5, and sample number 7. Maximum tensile strain of the samples number 7 and 5 decreased approximately 74.5% and 96%, respectively, compared to that of the raw material.

3.2 Micro-hardness

To determine the hardness of the samples (numbers 5 and 7), the measurements were performed at 5 points with an interval of 500 μm, in the center of the cross section (on the symmetry axis of the weld nugget). The measured hardness of the raw material (double-layer sheet), the sample number 5 and the sample number 7 are shown in Figure 5.

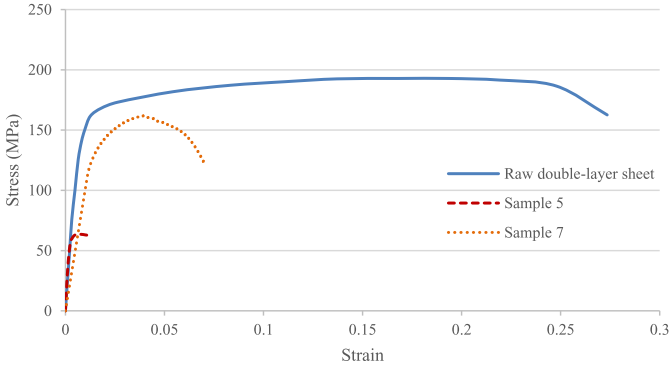

Fig. 4. Tensile stress-strain curves of the selected samples including the raw (non-welded) double-layer sheet, the sample welded by the thread tool in two passes from the Al side with rotational and traversing speeds of 800 rpm and 12 mm min^{-1} (sample number 5), and the sample welded by the conical tool in one pass from the Cu side with rotational and traversing speeds of 800 rpm and 12 mm min^{-1} (sample number 7).

According to the results, the existence of non-homogeneous intermetallic compounds in the SZ of the sample number 5 caused a non-uniform trend in the measured hardness values. Furthermore, significant increase in the hardness of this sample confirms the presence of the intermetallic phases, in comparison to the raw double-layer sheet.

In general, grain size, dislocation density, generated heat, and presence of intermetallic phases affect the hardness of the welding area [2]. Applying more welding passes can enhance the amount of the hardness in the welding zone [23]. Since the sample number 5 was welded by the threaded tool in two passes, more stirring and heat generation happened for a longer time, which lead to formation of more brittle phases. On the other hand, the sample number 7 was welded using the conical tool in one pass. The result exhibits that there is a more homogeneity in this sample (compared to the sample number 5) and the hardness values are more comparable to that of the raw double-layer sheet, although the presence of the intermetallic phases is possible.

Considering the results of the tensile tests and the values of the microhardness, an inverse relationship between these results can be observed. This could be due to the presence of the brittle intermetallic phases with high microhardness and low formability, resulting in a faster crack initiation and final fracture.

3.3 Microstructure

Different reasons such as difference in mechanical and physical properties of the employed material, adhesion of semi-solid material to tool surface, very high or very low temperature of the process, turbulence of the material, and material escaping (from the weld line) can lead to create some defects in the welding zone including kissing bonds and hooking defects. In addition, some channeling defects

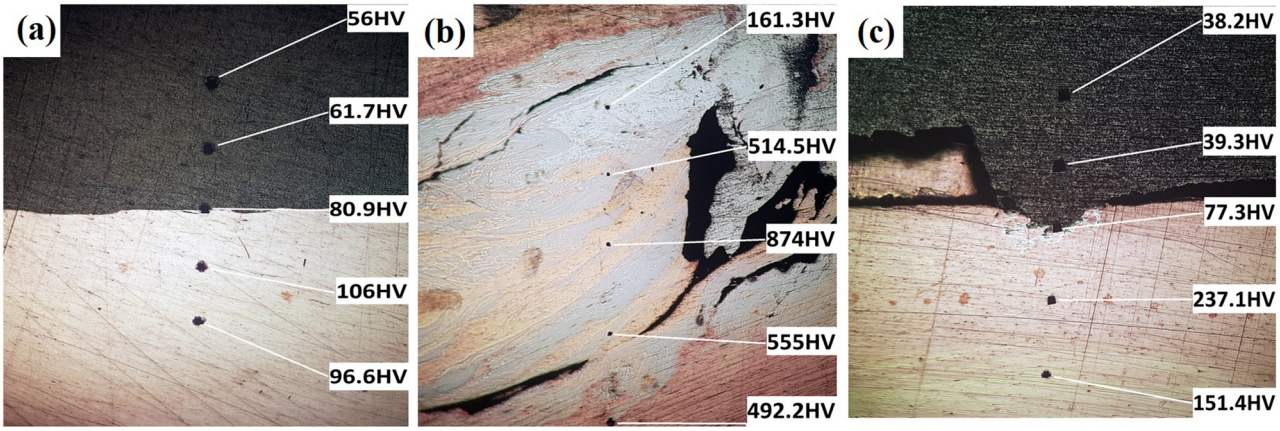

Fig. 5. The hardness of the different samples welded by (a) explosive welding (the raw double-layer sheet), (b) the thread tool in two passes from the Al side with rotational and traversing speeds of 800 rpm and 12 mm min^{-1} (sample number 5), (c) the conical tool in one pass from the Cu side with rotational and traversing speeds of 800 rpm and 12 mm min^{-1} (sample number 7).

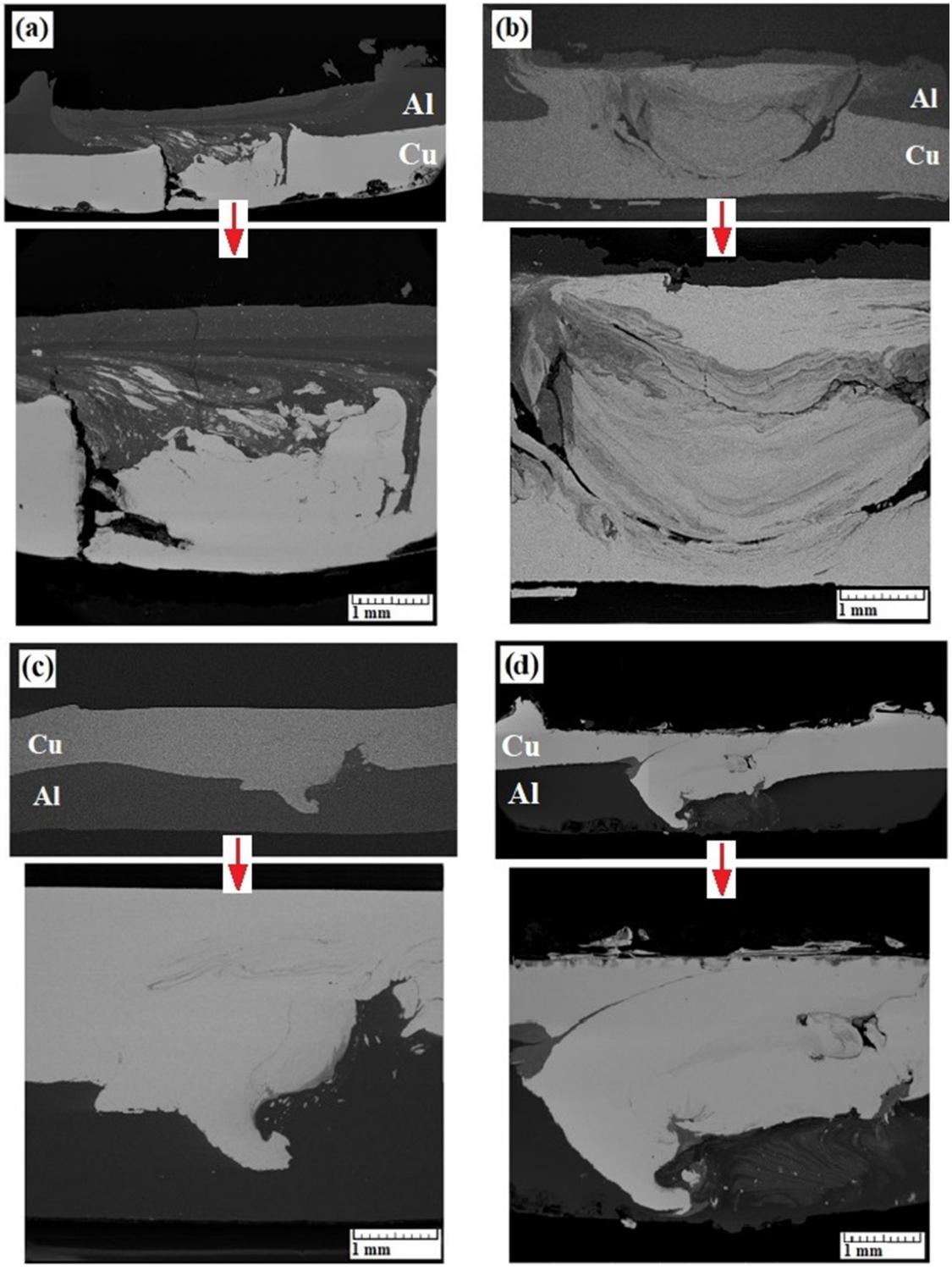

Fig. 6. Macro images of the samples welded by (a) the cylindrical tool in two passes from the Al side with rotational and traversing speeds of 800 rpm and 12 mm.min^{-1} (sample number 4), (b) the thread tool in two passes from the Al side with rotational and traversing speeds of 800 rpm and 12 mm.min^{-1} (sample number 5), (c) the conical tool in one pass from the Cu side with rotational and traversing speeds of 800 rpm and 12 mm.min^{-1} (sample number 7), (d) the conical tool in one pass from the Cu side with rotational and traversing speeds of 1250 rpm and 6 mm.min^{-1} (sample number 11).

could occur at the interface of the two materials due to the low temperature of the welding process. Macro images of the samples number 4, 5, 7, and 11 are shown in Figure 6. This figure indicates that except the sample number 7, other samples include different microstructural defects. More cavitation can be observed in the samples number 4

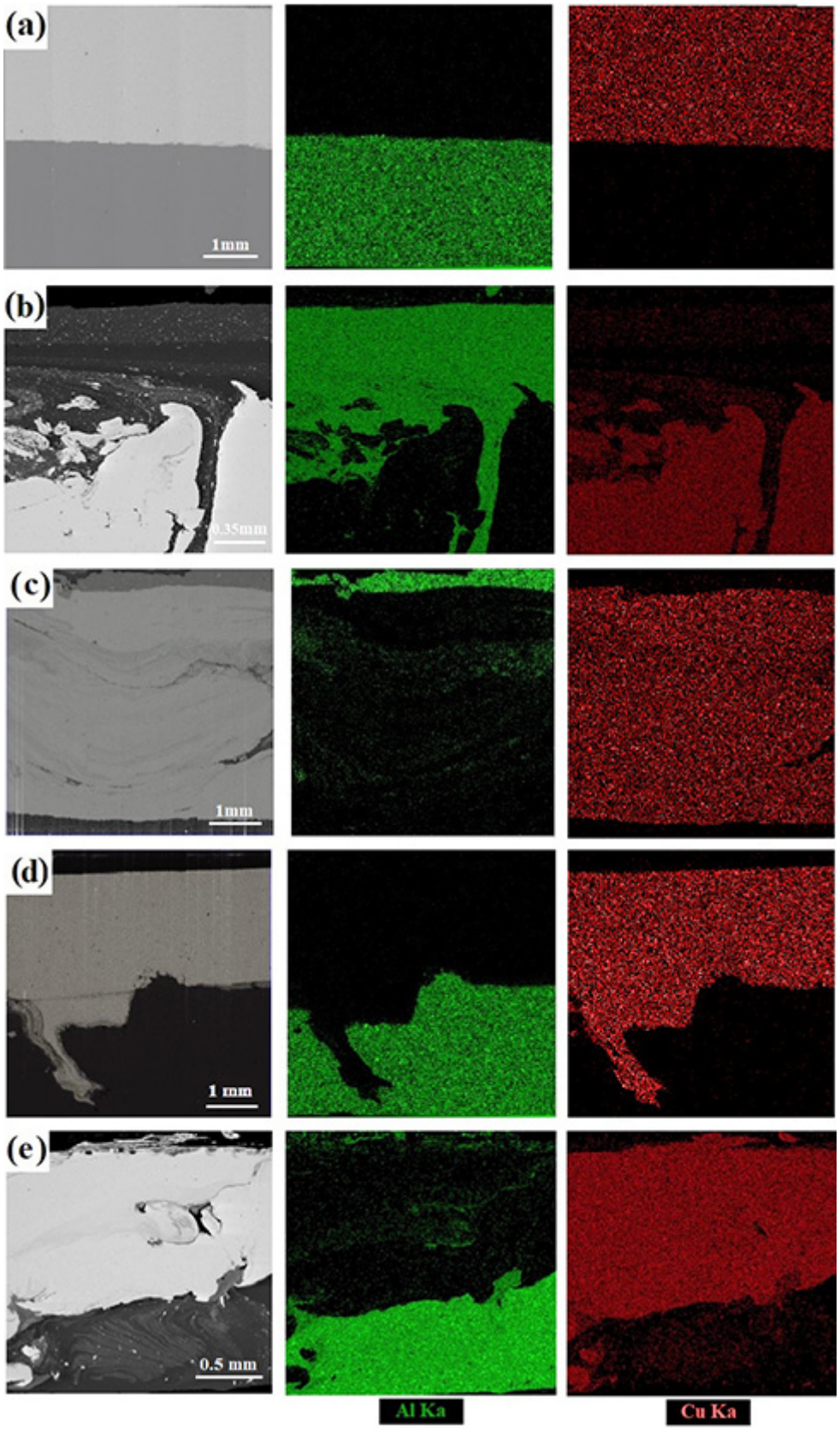

Fig. 7. Elemental map analysis of the samples welded by (a) explosive welding (the raw double-layer sheet), (b) the cylindrical tool in two passes from the Al side with rotational and traversing speeds of 800 rpm and 12 mm min^{-1} (sample number 4), (c) the thread tool in two passes from the Al side with rotational and traversing speeds of 800 rpm and 12 mm min^{-1} (sample number 5), (d) the conical tool in one pass from the Cu side with rotational and traversing speeds of 800 rpm and 12 mm min^{-1} (sample number 7), (e) the conical tool in one pass from the Cu side with rotational and traversing speeds of 1250 rpm and 6 mm min^{-1} (sample number 11).

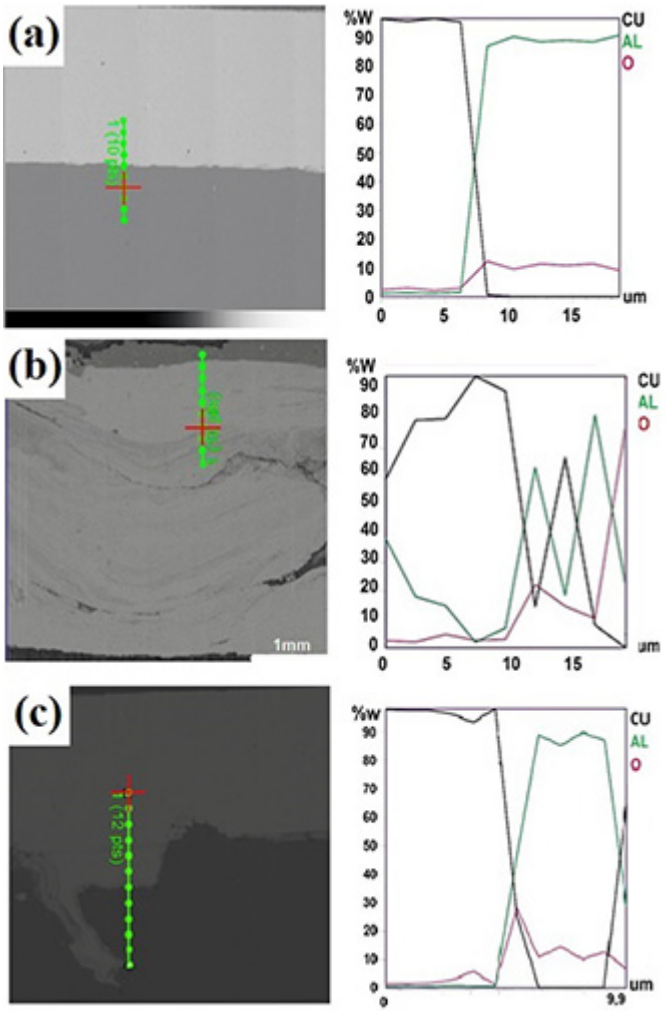

Fig. 8. Line scan analysis of the samples welded by (a) explosive welding (the raw double-layer sheet), (b) the thread tool in two passes from the Al side with rotational and traversing speeds of 800 rpm and 12 mm min^{-1} (sample number 5), and (c) the conical tool in one pass from the Cu side with rotational and traversing speeds of 800 rpm and 12 mm min^{-1} (sample number 7).

and 5, which the tool has penetrated from the Al side. These cavitation defects usually occurred in the areas between two metals and intermetallic phases due to the higher difference between the semi-solid temperatures and other properties of copper, aluminum, and their intermetallic compositions. More number of welding pass (samples number 4 and 5) and using the threaded tool (sample number 5) caused more defects. In higher temperatures of the welding, aluminum distributed into the copper sheet. After quenching, some cavities are formed in the interface of the different phases and materials. In fact, different shrinkage coefficients of the dissimilar materials especially at higher temperatures resulted in the formation of cavitation defects [13].

Figure 7 shows the elemental map analysis of the samples displayed in Figure 6. No obvious diffusion bonding can be observed in the raw double-layer sheet which was manufactured by the explosive welding process. Although the sample number 7 shows a very low amount of Al-Cu solution, the samples number 4, 5, and 11 exhibit a mixture of Al and Cu elements, which could lead to formation of more intermetallic phases. The presence of these brittle phases with different mechanical properties increases the microstructural defects before and during loading the joints and consequently decreases the tensile strength. Aluminum and copper were approximately completely mixed in the sample number 5, resulting in the least tensile strength. Using the threaded tool, entering from the Al side, applying two passes of welding and also higher rotational and less traversing speeds are the most possible reasons for this high amount of mixing, compared to the sample number 7.

Line scan analysis of the raw double-layer sheet, sample number 5, and sample number 7 are illustrated in Figure 8. Similar to Figure 7, a high amount of mixture can be observed in sample number 5, showing the presence of different intermetallic phases.

Regarding the literature, AlCu, Al_2Cu, and Al_4Cu_9 usually can be found in the Al-Cu FSW joint [24–26]. Different intermetallic regions of the sample number 5 and EDS analysis of them are shown in Figure 9. According to the atomic percentages of the elements in these regions, it could be concluded that the dominate phases in the regions A, B, C, D, and E are Al_4Cu_9, AlCu, Al_2Cu, Cu, and Al, respectively.

In Figure 10, the EDS analysis of the sample number 7 is illustrated for its different intermetallic regions. Atomic percentages of the elements in these regions shows that the presence of intermetallic phases of Al_2Cu and Al_4Cu_9 is more possible in the zones A and B. Moreover, Cu and Al are dominant in regions C and D, respectively.

4 Conclusion

The effects of friction stir welding parameters were investigated on the tensile strength of the welded double-layer sheets (produced by EXW method). Different welds by various parameters were carried out on the double-layer samples. Then, the uniaxial tensile behavior, microhardness, and microstructure of the samples were studied. The achievements of this research could be concluded as follows:

- Welding with conical tool, lower rotational and higher traversing speeds, Cu-side tool entrance, and in one pass led to achieve a higher tensile strength.
- The sample welded by the conical tool in one pass from the Cu side with rotational and traversing speeds of 800 rpm and 12 mm min^{-1} (sample number 7) offered the highest tensile strength of 161.35 MPa (equivalent to 84% of the UTS of the raw double-layer sheet). On the other hand, the samples welded by the thread tool in two passes from the Al side with rotational and traversing speeds of 800 rpm and 12 mm min^{-1} (sample number 5) exhibited the lowest UTS (64.5 MPa, equivalent to 33% of the UTS of the raw double-layer sheet).
- The most important reasons for UTS reduction could be attributed to the internal defects and formation of brittle intermetallic phases which happened due to the high temperature of the process. Employing the threaded tool,

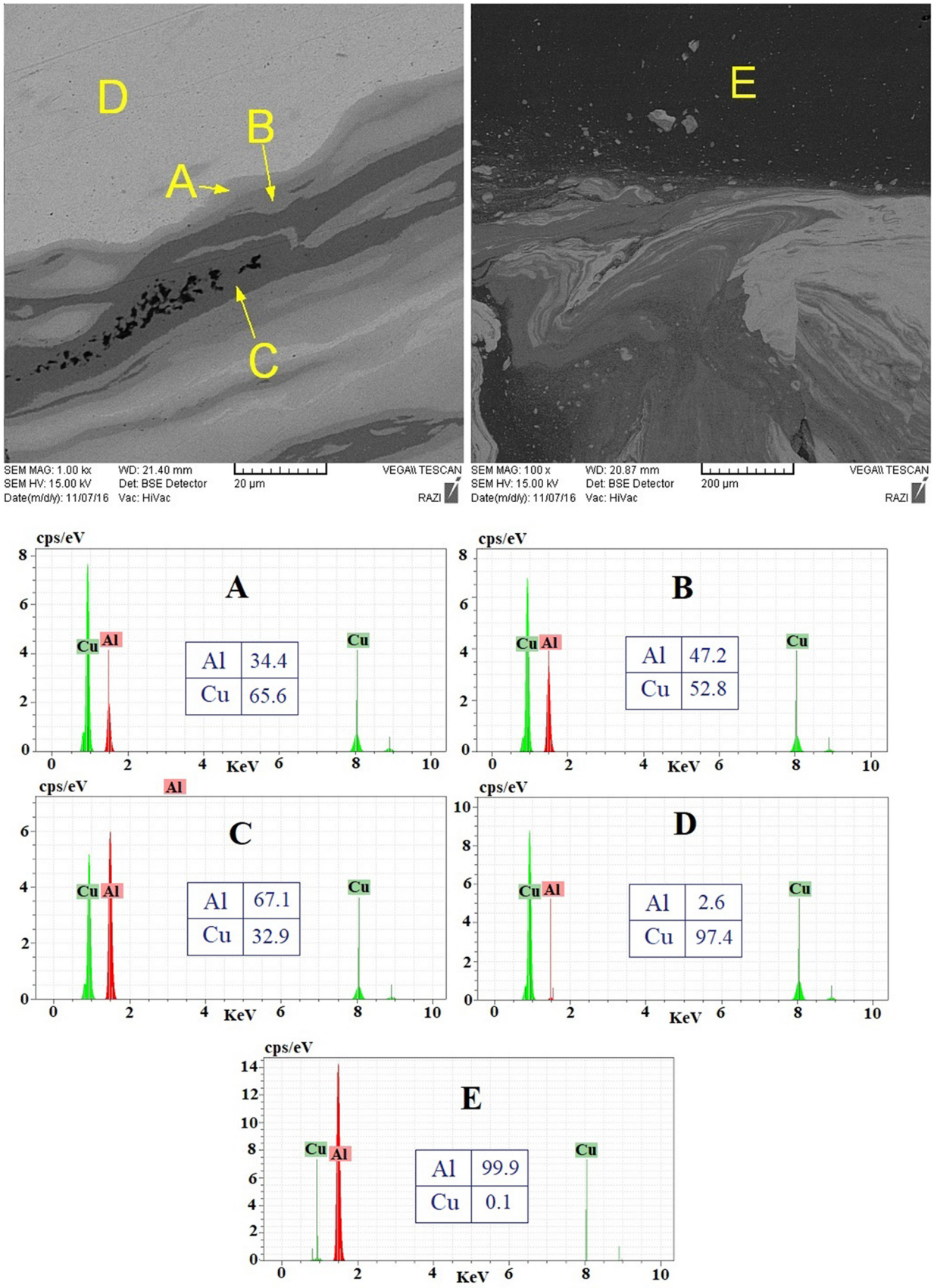

Fig. 9. Different intermetallic regions and EDS analysis of the sample welded by the thread tool in two passes from the Al side with rotational and traversing speeds of 800 rpm and 12 mm min^{-1} (sample number 5).

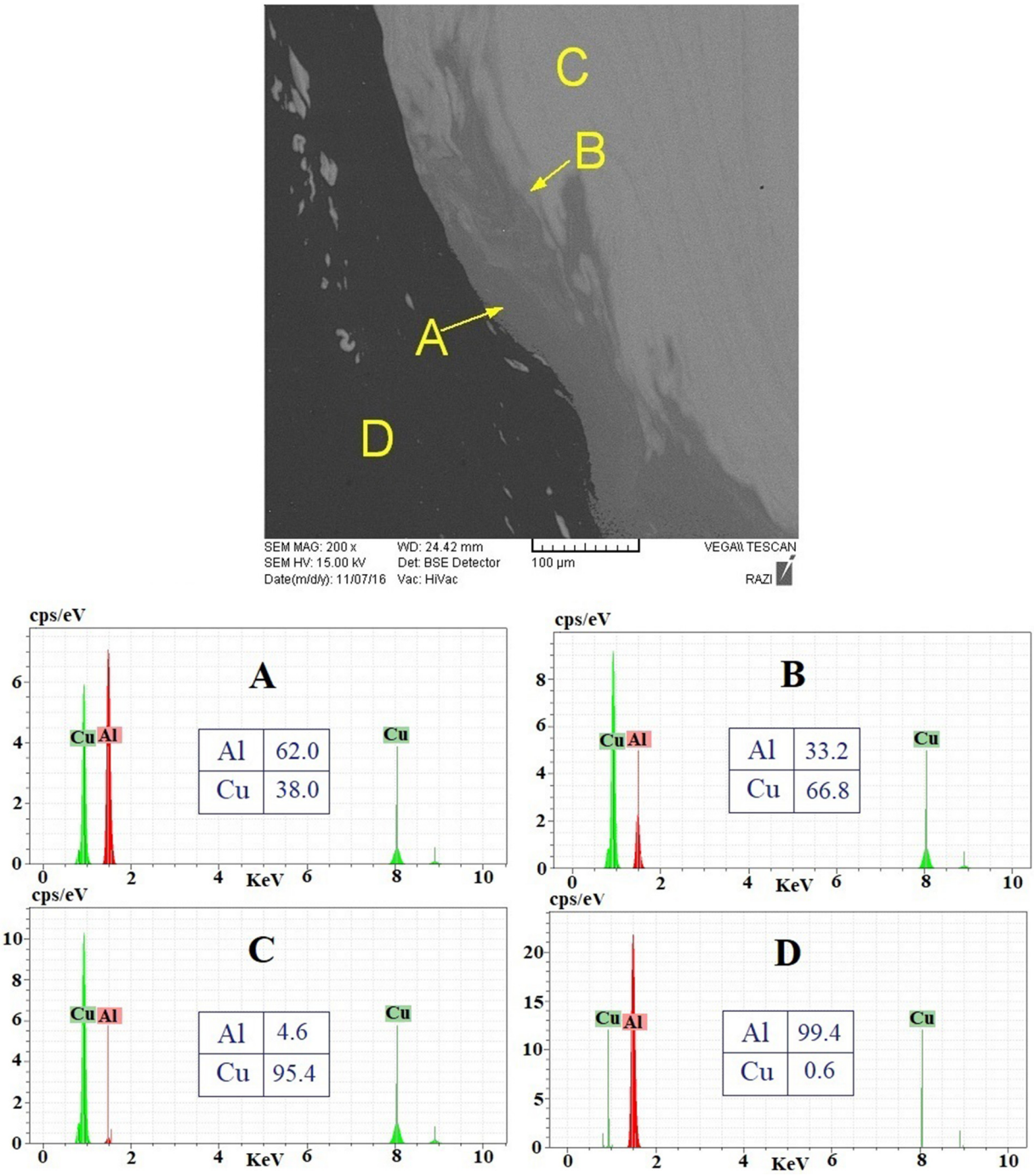

Fig. 10. Different intermetallic regions and EDS analysis of the sample welded by the conical tool in one pass from the Cu side with rotational and traversing speeds of 800 rpm and 12 mm.min^{-1} (sample number 7).

higher rotational and lower traversing speeds, entrance from the Al side, and applying more number of passes could generate more heat in the welding zone, resulting in increase of the temperature.

– Microhardness at the welding regions were mostly more than the base metals due to the presence of intermetallic phases and dynamic recrystallization process. The highest hardness was observed in the specimen with the least tensile strength (sample number 5) with a maximum value of 874 HV.
– While no obvious diffusion happened in the raw double-layer sheets, elemental map and line scan analysis showed that the aluminum and copper were approximately completely mixed in sample number 5, which led to formation of different intermetallic phases in this sample. On the other hand, the sample number 7 showed a very low amount of Al-Cu solution in the welding region.
– Microstructural evaluation indicated the presence of the intermetallic phases of Al_4Cu_9, AlCu, and Al_2Cu in the

sample number 5 and also Al_4Cu_9 and Al_2Cu in the sample number 7.

Nomenclature

ν Traversing speed ($mm\,min^{-1}$)
ω Rotational speed (rpm)
N Number of passes (–)

References

[1] W. Thomas, E. Nicholas, J. Needham, M. Murch, P. Templesmith, C. Dawes, Great Britain Patent Application No. 9125978.8. December, 1991

[2] A. Scialpi, M. De Giorgi, L. De Filippis, R. Nobile, F. Panella, Mechanical analysis of ultra-thin friction stir welding joined sheets with dissimilar and similar materials, Mater. Des. **29**, 928–936 (2008)

[3] S. Mironov, Y. Sato, H. Kokawa, H. Inoue, S. Tsuge, Structural response of superaustenitic stainless steel to friction stir welding, Acta Mater. **59**, 5472–5481 (2011)

[4] H.R. Shercliff, M.J. Russell, A. Taylor, T.L. Dickerson, Microstructural modelling in friction stir welding of 2000 series aluminium alloys, Mech. Ind. **6**, 25–35 (2005)

[5] N. Gangil, S. Maheshwari, A.N. Siddiquee, Influence of tool pin and shoulder geometries on microstructure of friction stir processed AA6063/SiC composites, Mech. Ind. **19** (2018)

[6] A. Jabbari, M. Sedighi, R. Vallant, A. Huetter, C. Sommitsch, Effect of pass number, rotational and traverse speed on particle distribution and microstructure of AZ31/SiC composite produced by friction stir processing, Key Eng. Mater., Trans Tech Publ. 765–770 (2015)

[7] H. Patle, R. Dumpala, B.R. Sunil, Machining characteristics and corrosion behavior of grain refined AZ91 mg alloy produced by friction stir processing: role of tool pin profile, Trans. Indian Inst. Metals. **71**, 951–959 (2018)

[8] R.S. Mishra, Z. Ma, Friction stir welding and processing, Mater. Sci. Eng. **50**, 1–78 (2005)

[9] A. Barcellona, G. Buffa, D. Contorno, L. Fratini, D. Palmeri, Microstructural changes determining joint strength in friction stir welding of aluminium alloys, Adv. Mater. Res. 591–598 (2005)

[10] M.M. Farahati, M. Abasi, S.H. Razavi, Welding Aluminum 1050 and Pure Copper using Friction Stir Welding (FSW), in *10th National Conference of Manufacturing Engineering. Babol, Iran*, 2009

[11] P. Xue, B.L. Xiao, D. Wang, Z. Ma, Achieving high property friction stir welded aluminium/copper lap joint at low heat input, Sci. Technol. Weld. Joining **16**, 657–661 (2011)

[12] X.-w. Li, D.-t. Zhang, Q. Cheng, W. Zhang, Microstructure and mechanical properties of dissimilar pure copper/1350 aluminum alloy butt joints by friction stir welding, Trans. Nonferrous Metals Soc. China **22**, 1298–1306 (2012)

[13] H. Bisadi, A. Tavakoli, M.T. Sangsaraki, K.T. Sangsaraki, The influences of rotational and welding speeds on microstructures and mechanical properties of friction stir welded Al5083 and commercially pure copper sheets lap joints, Mater. Des. **43**, 80–88 (2013)

[14] I. Galvão, D. Verdera, D. Gesto, A. Loureiro, D. Rodrigues, Influence of aluminium alloy type on dissimilar friction stir lap welding of aluminium to copper, J. Mater. Process. Technol. **213**, 1920–1928 (2013)

[15] H. Barekatain, M. Kazeminezhad, A. Kokabi, Microstructure and mechanical properties in dissimilar butt friction stir welding of severely plastic deformed aluminum AA 1050 and commercially pure copper sheets, J. Mater. Sci. Technol. **30**, 826–834 (2014)

[16] E.T. Akinlabi, A. Andrews, S.A. Akinlabi, Effects of processing parameters on corrosion properties of dissimilar friction stir welds of aluminium and copper, Trans. Nonferrous Metals Soc. China **24**, 1323–1330 (2014)

[17] E. Sadeghi, J. Shahbazi Karami, Investigation of mechanical properties of aluminum/copper joint using friction stir spot welding, Conference on new findings in aerospace and related fields. Tehran, Iran, 2015

[18] R. Anbukkarasi, S.V. Kailas, Role of third material (interlayer) on mechanical properties of the AA2024-copper joints carried out by friction stir welding (FSW), Trans. Indian Inst. Metals 1–4 (2019)

[19] F. Marandi, A. Jabbari, M. Sedighi, R. Hashemi, An Experimental, analytical, and numerical investigation of hydraulic bulge test in two-layer Al-Cu Sheets, J. Manufactur. Sci. Eng. **139**, 031005 (2017)

[20] A.R. Kumar, S. Varghese, M. Sivapragash, A comparative study of the mechanical properties of single and double sided friction stir welded aluminium joints, Proc. Eng. **38**, 3951–3961 (2012)

[21] K. Ramesh, S. Pradeep, V. Pancholi, Multipass friction-stir processing and its effect on mechanical properties of aluminum alloy 5086, Metall. Mater. Trans. A **43**, 4311–4319 (2012)

[22] A.F. Arezoudar, A. Hosseini, Optimization of friction stir welding parameters of dissimilar AA5052 and AA6061-T6 joint for achieving optimum microstructure and mechanical properties, Modares Mech. Eng. **17**, 20–30 (2017)

[23] M. Nazari, M.K.B. Givi, M.R. Farahani, J.M. Milani, H.M. Jamaliyan, Investigation on the effects of using Nano-size Al2O3 powder on the mechanical and microstructural in the multi-passes continuous friction stir welding of the 2024-T6, Modares Mech. Eng. **14** (2015).

[24] M.P. Mubiayi, E.T. Akinlabi, Evolving properties of friction stir spot welds between AA1060 and commercially pure copper C11000, Trans. Nonferrous Metals Soc. China **26**, 1852–1862 (2016)

[25] L. Zhou, R. Zhang, G. Li, W. Zhou, Y. Huang, X. Song, Effect of pin profile on microstructure and mechanical properties of friction stir spot welded Al-Cu dissimilar metals, J. Manufactur. Process. **36**, 1–9 (2018)

[26] A. Boucherit, M.-N. Avettand-Fènoël, R. Taillard, Effect of a Zn interlayer on dissimilar FSSW of Al and Cu, Mater. Des. **124**, 87–99 (2017)

Cite this article as: M.T. Tabrizi, A.J. Mostahsan, M. Sedighi, Effects of process parameters on tensile strength of friction stir welded Al-Cu double-layer sheets, Mechanics & Industry **21**, 503 (2020)